Front. Optoelectron. 2017, 10(4): 363–369
DOI 10.1007/s12200-017-0728-2

RESEARCH ARTICLE

Diluted magnetic characteristics of Ni-doped AlN films via ion implantation

Chong ZHAO, Qixin WAN, Jiangnan DAI (✉), Jun ZHANG, Feng WU, Shuai WANG, Hanling LONG, Jingwen CHEN, Cheng CHEN, Changqing CHEN

Wuhan National Laboratory for Optoelectronics, Huazhong University of Science and Technology, Wuhan 430074, China

© Higher Education Press and Springer-Verlag Berlin Heidelberg 2017

Abstract The structural and magnetic properties, as well as the mechanism of magnetization, of Ni-implanted AlN films were studied. AlN was deposited on Al_2O_3 substrates by metalorganic chemical vapor deposition (MOCVD), and subsequently Ni ions were implanted into the AlN films by Metal Vapor Arc (MEVVA) sources at an energy of 100 keV for 3 h. The films were annealed at 900°C for 1 h in the furnace in order to transfer the Ni ions from interstitial sites to substitutional sites in AlN, thus activating the Ni^{3+} ions. Characterizations were performed *in situ* using X-ray diffraction (XRD), X-ray photoemission spectroscopy (XPS), and vibrating sample magnetometry (VSM), which showed that the films have a wurtzite structure without the formation of a secondary phase after implanting and annealing. Ni ions were successfully implanted into substitutional sites of AlN films, and the chemical bonding states are Ni-N. The apparent hysteresis loops prove that the films exhibited magnetism at 300 K. The room temperature (RT) saturation magnetization moment (M_s) and coercivity (H_c) values were about 0.36 emu/g and 35.29 Oe, respectively. From the first-principles calculation, a total magnetic moment of 2.99 μB per supercell is expected, and the local magnetic moment of a NiN_4 tetrahedron, 2.45 μB, makes the primary contribution. The doped Ni atom hybridizes with four nearby N atoms in a NiN_4 tetrahedron; then the electrons of the N atoms are spin-polarized and couple with the electrons of the Ni atom with strong magnetization, which results in magnetism. Therefore, the p-d exchange mechanism between Ni-3d and N-2p can be the origin of the magnetism. It is expected that these room temperature, ferromagnetic, Ni-doped AlN films will have many potential applications as diluted magnetic semiconductors.

Received April 12, 2017; accepted July 13, 2017

E-mail: daijiangnan@hust.edu.cn

Keywords III-V nitrides, metalorganic chemical vapor deposition (MOCVD), diluted magnetic semiconductors, first-principles

1 Introduction

III-nitride semiconductor material has a direct wide bandgap, good structural, chemical, and thermal stability, good light transmission characteristics, and low toxicity, which gives it great potential value as a diluted magnetic semiconductor (DMS). DMS materials have attracted considerable interest because of their potential applications in spintronic applications [1,2]. Since the original discovery of magnetism in Mn-doped GaAs at a temperature of 100 K [3,4], III-V based DMSs have been widely investigated [5–8]. Among them, AlN has attracted much attention as a promising DMS because of its stable mechanical properties, wide band-gap, and high Curie temperature (T_c). It is predicted that transition-metal-doped AlN is ferromagnetic above room temperature (RT) [9,10]. Up until now, Mg-, Mn-, Co-, Cr-, Cu-, Mg- and Fe-doped AlN with RT magnetism have been reported [11–15]. However, Ni-doped AlN DMSs are rarely studied because the Ni clusters are easily precipitated in the semiconductors [16]. A series of problems have to be solved to enable actual applications. For example, it is difficult to prepare the RT ferromagnetic materials. Furthermore, the origin of the magnetism in transition metal (TM)-doped AlN DMSs is still debatable. For use in practical applications, Ni-doped AlN DMSs with room temperature magnetism are necessary [17,18]. This work focused on the most intensively investigated III-nitride semiconductor material: AlN films. Theoretical and experimental research was conducted on the Ni-doped AlN diluted magnetic semiconductors.

In this work, we focused on the most intensively investigated III-nitride semiconductor material: AlN films.

The Ni-doped AlN diluted magnetic semiconductors were studied by theoretical and experimental methods. The structure, magnetic properties, and mechanism of magnetization of Ni-implanted AlN films were studied. The analysis shows that the Ni-implanted AlN films have a wurtzite structure without the formation of a secondary phase after annealing; this facilitates the transfer of Ni ions from interstitial sites to substitutional sites. The magnetic measurement indicates that the Ni-doped AlN films exhibited magnetism at 300 K. The p-d exchange mechanism is also discussed in detail from the first-principles calculation.

2 Experimental

AlN films were prepared on sapphire substrates by metalorganic chemical vapor deposition (MOCVD). The samples were grown on c-sapphire substrates in a vertical cold wall MOCVD reactor under a pressure of 40 Torr. Trimethylaluminum (TMAl) and ammonia were used as precursors for the Al and N sources, and H_2 was used as carrier gas. First, a thin high-temperature AlN (HT-AlN) film, around 60 nm thick, was deposited on the sapphire substrate via the pulsed atomic layer epitaxy (PALE) technique, with TMAl and ammonia flowing into the growth chamber separately at 1050°C. Subsequently, an AlN intermediate layer with a thickness of 20 nm was deposited at 870°C while TMAl and ammonia were introduced into the chamber simultaneously. Then HT-AlN, around 300 nm thick, was deposited using the same growth conditions as the HT-AlN grown initially. The as-grown AlN film will be designated in this paper as “Sample a”. A high purity (5N) nickel target with a diameter of 10 mm was used for Ni implantation by Metal Vapor Arc (MEVVA) sources at an implantation energy of 100 keV at 300 K for 3 h. The base pressure in the chamber was below 3.5×10^{-3} Pa and the injection dose was 3×10^{17} ion/cm^2. Subsequently, the Ni implanted sample was divided into two parts. One was kept to study in the as-implanted state (designated as “Sample b before annealing”) while the other one was annealed at 900°C under a pressure of 840 Pa in the furnace to repair the crystal lattice of the AlN film and to activate the Ni ions (designated as “Sample b after annealing”). The gas flow rate was 1 L/min of N_2, and the sample was positioned face-down to avoid the formation of secondary Ni phases such as NiO and Ni_2O_3. The annealing time was 1 h.

Chemical compositions were measured by X-ray photoemission spectroscopy (XPS, Kratos Amicus, Manchester, UK). Structural properties were determined by X-ray diffraction (XRD, Rigaku D/Max-A, Cu Kα), and magnetic properties were investigated with a vibrating sample magnetometer (VSM) in the temperature range of 900 K. Before the measurement, we used acetone solution, alcoholic solution, and deionized water (in chronological order) to clean the samples and thereby minimize any false artifacts from contaminants.

3 Results and discussion

Figure 1 shows the XRD spectra for three AlN films. Sample a has a significant diffraction peak at 36.09°, which corresponds to the peak value of AlN (002). There is no other impurity peak in Sample a, which shows that the AlN epitaxial thin film is of high purity. In contrast to Sample a, Sample b has a diffraction peak at 35.97° corresponding to the AlN (002) peak and an additional peak at 44.4° corresponding to the peak of metallic Ni, which indicates that Ni ions were successfully implanted into the AlN epitaxial film and some Ni ions may be present at the interstitial sites of the film after ion implantation. Just as in the case of Sample a, we can only see one obvious peak at 36.05° in Sample b after annealing, without any Ni metal peak, which shows that Sample b after annealing has the wurtzite structure without any other impurity phases, such as NiO and Ni_2O_3. It is speculated that Ni ions may shift from the interstitial sites to the substitution sites of the crystal lattice.

To study the influence of Ni ion implantation on the lattice constants of AlN thin films, the AlN (002) diffraction peaks in Fig. 1 were analyzed. It is not difficult to find that the AlN (002) diffraction peak in Sample b before annealing shifted to a lower angle than that of Sample a, which indicates that the lattice constant of the AlN film enlarged slightly as the Ni ions were implanted into the AlN film. This is mainly because Ni ions incorporated into the interstitial sites in the AlN film and

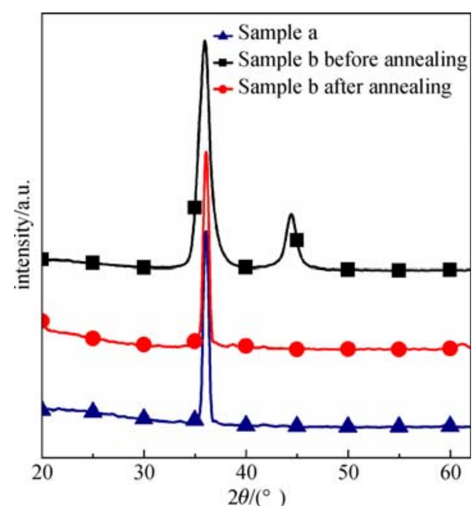

Fig. 1 XRD spectra for the as grown AlN film, Ni-implanted AlN film before annealing and Ni-implanted AlN film after annealing

increased the lattice stress, which led to the lattice expansion. The AlN (002) peak (36.05°) in Sample b after annealing is higher than that (35.97°) in Sample b before annealing, indicating that the lattice of the AlN film has contracted slightly after annealing at 900°C. This result is similar to that reported by Pan et al. [19], who found that Si ions were successfully doped into the substitutional sites in the AlN thin films. In our present experiment, Ni ions transferred from interstitial sites to substitutional sites of AlN after annealing; thus, Ni no longer occupied the interstitial sites in the form of metal particles, causing the shrinkage of the lattice spacing. Compared to Sample a, it can be seen that the AlN (002) diffraction peak of Sample b shifted to the left after annealing. That is to say, the lattice spacing is slightly enlarged. This is because the radius of Ni ions is larger than that of Al ions, and the Ni-N bond is longer than the Al-N bond. Therefore, Ni^{3+} occupying the location of Al^{3+} can cause the expansion of lattice constants of AlN film after the annealing treatment. This indicates that the annealing treatment at 900°C is facilitates the transfer of Ni ions from interstitial sites to substitutional sites of AlN and activates the Ni^{3+} ions.

XPS is largely used for surface characterization, and it can provide valuable information on the chemical state of ions. The XPS measurements were performed with a Kratos Axis Ultra DLD with the monochromatic Al Kα line (1486.7 eV). An analyzer pass energy of 100 eV with a 1 eV energy step was usually used to obtain high resolution photoelectron spectra. Large X-ray spots (500 μm) were used to explore the surface. To further analyze the valence states and the chemical bonding states of Ni and Al, XPS measurements of Sample b before and after annealing were carried out. Figure 2 shows the Ni-2p and Al-2p high-resolution XPS spectra of Sample b. The Gaussian method was used to fit the XPS spectra, and the C-1s line at 285.2 eV was used to calibrate the binding energies. The single peak of Al-2p occurs at 74.1 eV in Fig. 2(a), which corresponds to Al^{3+}-$2p_{3/2}$ in the AlN wurtzite structure. This indicates that Al ions mainly exist in the Al^{3+} state, and the chemical bonding states are Al-N, rather than some other state, such as Al-Ni or Al_i. These results show that the Ni ion implantation and annealing treatment have little effect on the valence and chemical bonding states of Al in Ni-doped AlN films.

Figure 2(b) shows that the peaks of Ni-2p in Sample b before annealing are at 852.6 and 869.8 eV, which correspond to Ni metal $2p_{3/2}$ and Ni metal $2p_{1/2}$, respectively. These results show that Ni ions mainly exist in the form of Ni metal particles and the chemical bonding states are Ni-Ni. We believe that Ni ions were successfully implanted into the AlN epitaxial thin film and existed in the interstitial state before annealing. This result is consistent with the results of XRD analysis.

After annealing, the peaks of Ni-2p at 855.2, 860.7, and 873.0 eV can be observed in the XPS spectra of Sample b. Since the peaks at 852.6 and 869.8 eV corresponding to metallic Ni were not observed in Sample b after annealing, the presence of Ni metal clusters can be excluded. Since the Ni-$2p_{3/2}$ and Ni-$2p_{1/2}$ peaks of NiO are located at 853.3 and 871.7 eV, respectively [20], which does not correspond to the peaks in Sample b, the chemical bonding states of Ni-O can be ruled out. The distance between Ni-$2p_{3/2}$ (855.2 eV) and Ni-$2p_{1/2}$ (873.0 eV) peaks is 17.8 eV, which is distinctly different from that of NiO (18.4 eV). This further indicates that NiO does not existed in Sample b after annealing.

The Ni-$2p_{3/2}$ (855.2 eV) and Ni-$2p_{1/2}$ (873.0 eV) correspond well with that for Ni^{3+}-$2p_{3/2}$ as described in Ref. [21]. To further deduce whether the chemical bonding state of Ni^{3+} is Ni-O or Ni-N, the magnetization versus magnetic field (*M-H*) loop measurements for Sample b were conducted, as shown in Fig. 3. The results show that Sample b has high temperature magnetic properties after annealing, whereas Ni_2O_3 is paramagnetic, indicating that Ni_2O_3 is not present in Sample b. Moreover, the peak of

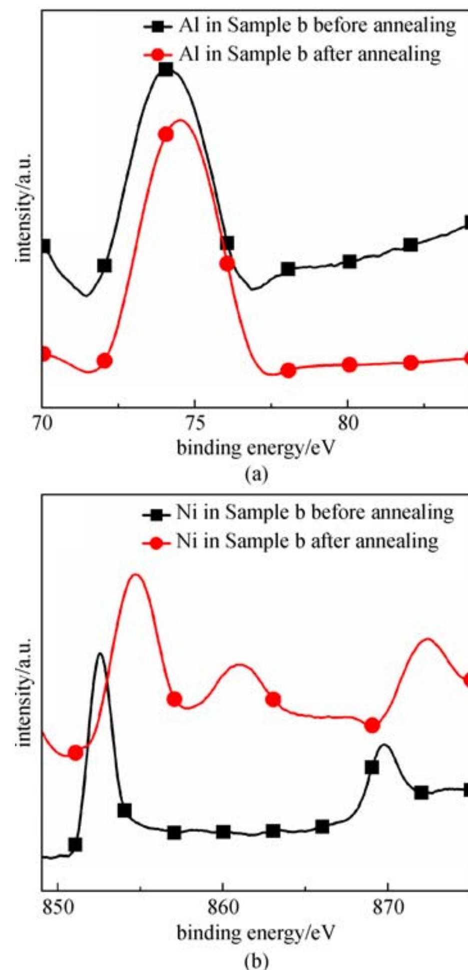

Fig. 2 (a) Al-2p and (b) Ni-2p high-resolution XPS spectra of Sample b before and after annealing

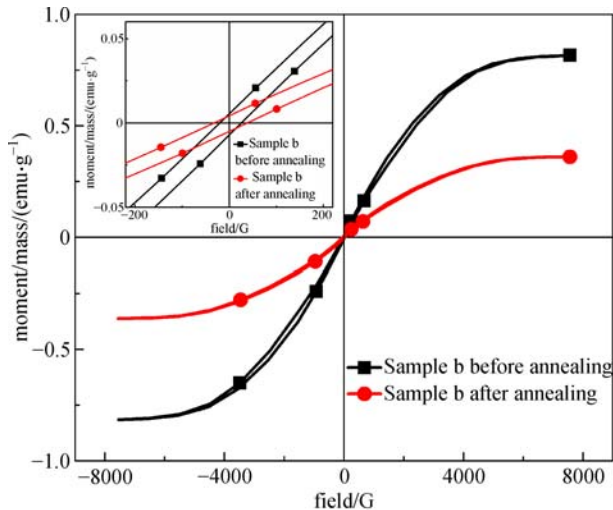

Fig. 3 Magnetization versus magnetic field (*M-H*) loops for Sample b before and after annealing

Ni-2p of Ni_2O_3 is 855.8 eV, which does not correspond to the peaks in Sample b after annealing; therefore, the presence of Ni_2O_3 can be ruled out. Hence, it is presumed that the Ni atoms were successfully implanted into the AlN epitaxial thin films, and Ni^{3+} ions were incorporated into substitutional sites after annealing. Furthermore, the chemical bonding state of Ni^{3+} is Ni-N in all probability, rather than Ni-O. It is suggested that the annealing treatment can assist Ni ions to transfer from interstitial sites to substitutional sites of AlN and activate the Ni^{3+} ions, which is consistent with the analysis of the XRD pattern of Sample b after annealing.

To study the magnetic properties of Ni-doped AlN films, the type-b samples were analyzed with a VSM. An external magnetic field of 8000 Oe was applied parallel to the AlN surface at 300 K to measure the magnetization versus magnetic field (*M-H*) loops of these b-type samples. The diamagnetic properties of pure AlN film were subtracted from the DMS magnetization measurements. As presented in Fig. 3, the apparent hysteresis loops of Sample b were clearly observed, which proves that these films have magnetism at 300 K. The saturation magnetization moment (M_s) and coercivity (H_c) values were also measured.

For Sample b before annealing, M_s is 0.82 emu/g and H_c is 22.8 Oe. From the analysis of the XRD and XPS measurements, it is known that metallic Ni particles exist in Sample b before annealing. The magnetic properties of Sample b before annealing are mainly attributed to Ni metal in the AlN film because of the obvious magnetic properties of metallic Ni. The M_s of Sample b after annealing is 0.36 emu/g and the H_c is 35.29 Oe; in other words, the M_s is weakened after annealing. Since only Ni ions were introduced to the AlN film and there are no Ni clusters existing in Sample b after annealing, the long distance between Ni ions makes it impossible for any direct interaction to occur, which shows that the magnetism is not due to Ni clusters. Simultaneously, because of the high resistivity of AlN films at RT, free-carrier mediated models are not suitable for explaining the magnetism. After annealing, Ni ions transfer from interstitial sites to substitutional sites of AlN and the chemical bonding states are Ni-N. The magnetism may be derived from Ni-N in NiN_4 tetrahedron. However, the mechanism of magnetization is still indeterminate, and further research is needed.

It is worth noting that the H_c of Sample b after annealing at RT is higher than that of bulk Ni (6 Oe) [22] and lower than that of Ni-doped AlN DMSs (about 40 Oe) [18]. The coercivity of Sample b after annealing is relatively low, which is more suitable for spin processing. Sample b has high magnetization after annealing at 900°C, which also shows that Ni-doped AlN thin film is a promising DMS material.

To further understand the mechanism of magnetization of Ni-doped AlN, the spin-polarized partial density of states (DOS) of Ni-doped AlN was analyzed from a first-principles study, and was calculated by using the Vienna ab-initio simulation package (VASP). The AlN was created from a 32-atom (2 × 2 × 2) supercell of $Al_{16}N_{16}$ having the wurtzite structure. One Al atom and one N atom in the supercell were respectively replaced by a Ni atom to study their formation energy. Since the radius and ionicity of Ni is closer to that of Al, than N, it is expected that Ni will be inclined to occupy Al sites in the AlN film. Indeed, the formation energy of Ni_{Al} in Ni-doped AlN is 7.02 eV lower than that of Ni_N, which shows that Ni prefers to occupy the Al site. Figure 4 shows the total DOS of $Al_{16}N_{16}$ and $Al_{15}NiN_{16}$, where the Fermi level is set to zero. The

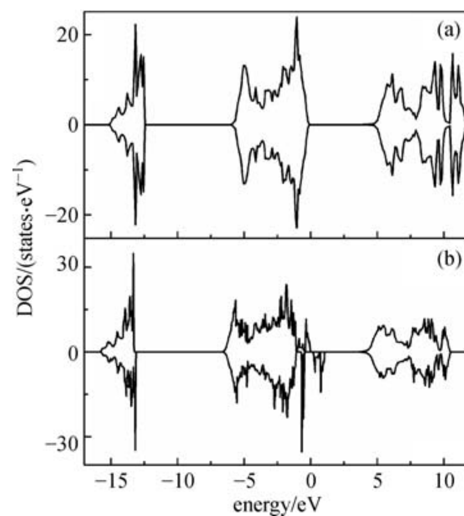

Fig. 4 Total DOS of (a) $Al_{16}N_{16}$ and (b) $Al_{15}NiN_{16}$. Fermi level is set to zero. Positive (negative) values correspond to the majority (minority) spin

majority-spin channel and the minority-spin channel of AlN are completely symmetric in Fig. 4(a), which shows the AlN is nonmagnetic. This result is in keeping with the experimental research. Figure 4(b) shows the total spin DOS of $Al_{15}NiN_{16}$. The valence band is in the range of $-16 \sim -13$ eV and $-6.6 \sim 0$ eV. By comparing the total DOS of $Al_{15}NiN_{16}$ and $Al_{16}N_{16}$, it can be found that the d electron of impurity Ni introduces a new impurity level near the Fermi surface. The majority-spin channel is not completely coincident with the minority-spin channel. This indicates that the Ni-doped AlN film is magnetic, which is in accord with our previous analysis of the magnetization measurements.

To further analyze the mechanism of magnetization of Ni-doped AlN, partial DOS of Al-3d, Ni-3d and N-2p are shown in Fig. 5. In the majority-spin channel, the peaks of Ni-3d at -3.40, -2.30, -1.29, -0.86, and -0.34 eV overlap with that of N-2p. In the minority-spin channel, the Fermi level passes through the overlapped band of Ni-3d and N-2p. These characteristics manifest a very strong hybridization between a Ni atom and four nearby N atoms in a NiN_4 tetrahedron, which induces the magnetization of Ni and N atoms. A total magnetic moment of 2.99 μB per supercell is calculated; and the local magnetic moment of Ni (1.65 μB) makes the primary contribution. The contribution of the N atom at the top site of the NiN_4 tetrahedron is 0.17 μB, which is less than that of the other three N atoms lying in the basal plane of the NiN_4 tetrahedron (0.21 μB). This is because the Ni–N bond of the N atom at the top site is longer than that of the other three N atoms. Analyzing the magnetic moments, we found that a majority of the magnetic moments are contributed by the NiN_4 tetrahedron. The doped Ni atom hybridizes with four nearby N atoms in a NiN_4 tetrahedron; then electrons of the N atoms are spin-polarized and couple with electrons of the Ni atom with strong magnetization, which results in magnetism. Therefore, the p-d exchange mechanism between Ni-3d and N-2p can be the origin of the magnetism.

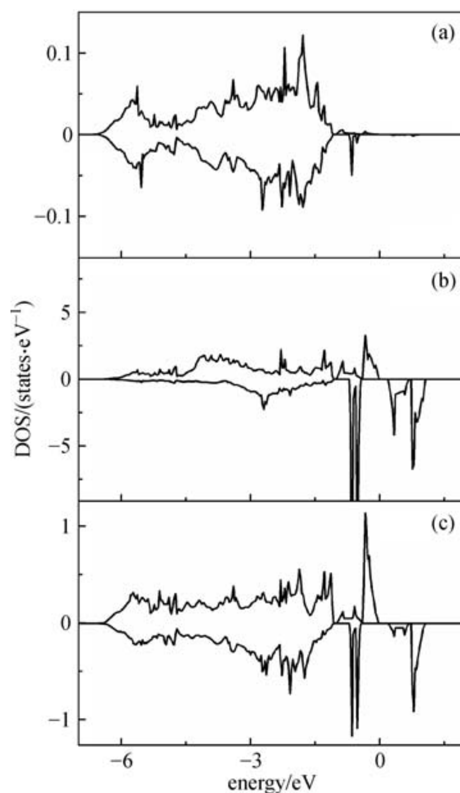

Fig. 5 Spin DOS of (a) Al-3d, (b) Ni-3d and (c) N-2p of AlN. Fermi level is set to zero. Positive (negative) values correspond to the majority (minority) spin

4 Conclusions

In summary, we reported on the structure, elemental valences, and magnetic properties of Ni-doped AlN films that were fabricated by ion implantation. The AlN films had been deposited on Al_2O_3 substrates by MOCVD. The annealing treatment at 900°C facilitated the transfer of Ni ions from interstitial sites to substitutional sites of AlN and activated the Ni^{3+} ions. The Ni-doped AlN films after annealing have a wurtzite structure without any secondary phase having been formed, as confirmed by the XRD, XPS, and *M-H* measurements. The RT, M_s and H_c obtained are about 0.36 emu/g and 35.29 Oe, respectively. Sample b exhibited magnetism at 300 K after annealing. A first-principles calculation suggests that the p-d exchange mechanism between Ni-3d and N-2p can be the origin of the magnetism. It is expected that the room temperature ferromagnetic Ni-doped AlN films will have many potential applications as diluted magnetic semiconductors.

Acknowledgements This work was supported by the National Key R&D Program of China (Nos. 2016YFB0400901, and 2016YFB0400804), the Key Laboratory of Infrared Imaging Materials and Detectors, Shanghai Institute of Technical Physics, Chinese Academy of Sciences (No. IIMDKFJJ-15-07), the National Natural Science Foundation of China (Grant Nos. 61675079, 11574166, and 61377034), and the Director Fund of WNLO.

References

1. Ohno H, Shen A, Matsukura F, Oiwa A, Endo A, Katsumoto S, Iye Y. (Ga,Mn)As: a new diluted magnetic semiconductor based on GaAs. Applied Physics Letters, 1996, 69(3): 363–365
2. Philip J, Theodoropoulou N, Berera G, Moodera J S, Satpati B. High-temperature ferromagnetism in manganese-doped indium-tin oxide films. Applied Physics Letters, 2004, 85(5): 777–779
3. Litvinov V I, Dugaev V K. Ferromagnetism in magnetically doped III–V semiconductors. Physical Review Letters, 2001, 86(24): 5593–5596
4. Rode K, Anane A, Mattana R, Contour J P, Durand O, LeBourgeois R. Magnetic semiconductors based on cobalt substituted ZnO. Journal of Applied Physics, 2003, 93(10): 7676–7678

5. Vetter U, Zenneck J, Hofsass H. Intense ultraviolet cathodoluminescence at 318 nm from Gd^{3+}-doped AlN. Applied Physics Letters, 2003, 83(11): 2145–2147
6. Han S Y, Hite J, Thaler G T, Frazier R M, Abernathy C R, Pearton S J, Choi H K, Lee W O, Park Y D, Zavada J M, Gwilliam R.Effect of Gd implantation on the structural and magnetic properties of GaN and AlN. Applied Physics Letters, 2006, 88(4): 042102
7. Luo J T, Li Y Z, Kang X Y, Zeng F, Pan F, Fan P, Jiang Z, Wang Y. Enhancement of room temperature ferromagnetism in Cu-doped AlN thin film by defect engineering. Journal of Alloys and Compounds, 2014, 586(4): 469–474
8. Xiong J, Guo P, Cai Y, Stradel B, Brumek J, He Y, Gua H. Structural, magnetic and nanomechanical properties in Ni-doped AlN films. Journal of Alloys and Compounds, 2014, 606: 55–60
9. Nepal N, Bedair S M, Elmasry N A, Lee D S, Steckl A J, Zavada J M. Correlation between compositional fluctuation and magnetic properties of Tm-doped AlGaN alloys. Applied Physics Letters, 2007, 91(22): 222503
10. Shi C, Qin H, Zhang Y, Hu J F, Ju L. Magnetic properties of transition metal doped AlN nanosheet: first-principle studies. Journal of Applied Physics, 2014, 115(5): 053907
11. Frazier R M, Stapleton J, Thaler G T, Abernathy C R, Pearton S J, Rairigh R, Kelly J, Hebard A F, Nakarmi M L, Nam K B, Lin J Y, Jiang H X, Zavada J M, Wilson R G. Properties of Co-, Cr-, or Mn-implanted AlN. Journal of Applied Physics, 2003, 94(3): 1592–1596
12. Wu R Q, Peng G W, Liu L, Feng Y P, Huang Z G, Wu Q Y. Ferromagnetism in Mg-doped AlN from *ab initio* study. Applied Physics Letters, 2006, 89(14): 142501
13. Shi L J, Zhu L F, Zhao Y H, Liu B G. Nitrogen defects and ferromagnetism in Cr-doped dilute magnetic semiconductor AlN from first principles. Physical Review B: Condensed Matter, 2008, 78(19): 195206
14. Ran F Y, Subramanian M, Tanemura M, Hayashi Y, Hihara T. Ferromagnetism in Cu-doped AlN films. Applied Physics Letters, 2009, 95(11): 112111
15. Xiong J, Guo P, Guo F, Sun X L, Gu H S. Room temperature ferromagnetism in Mg-doped AlN semiconductor films. Materials Letters, 2014, 117(117): 276–278
16. Pan D, Jian J K, Ablat A, Li J, Sun Y F, Wu R. Structure and magnetic properties of Ni-doped AlN films. Journal of Applied Physics, 2012, 112(5): 053911
17. Sato K, Katayama Y H. Ferromagnetism in a transition metal atom doped ZnO. Physica E, Low-Dimensional Systems and Nanostructures, 2001, 10(1–3): 251–255
18. Wang Q, Sun Q, Jena P, Kawazoe Y. Carrier-mediated ferromagnetism in N codoped (Zn, Mn) O thin films. Physical Review B: Condensed Matter and Materials Physics, 2004, 70(5): 052408
19. Pan D, Jian J K, Sun Y F, Wu F. Structure and magnetic characteristics of Si-doped AlN films. Journal of Alloys and Compounds, 2012, 519(7): 41–46
20. Wagner C D, Riggs W M, Davis L E, Moulder J F, Muilenberg G E. Handbook of X-ray Photoelectron Spectroscopy. Minnesota: Perkin-Elmer Corporation Press, 1979, 80–81
21. Stainton M P. Syringe procedure for transfer of nanogram quantities of mercury vapor for flameless atomic absorption spectrophotometry. Analytical Chemistry, 1971, 43(4): 625–627
22. Cho J H, Hwang T J, Joh Y G, Kim E C, Kim D G H, Lee K J, Park H W, Ri H C, Kim J P, Cho C R. Room-temperature ferromagnetism in highly-resistive Ni-doped TiO_2. Applied Physics Letters, 2006, 88(9): 092505

Chong Zhao received the B.E. degree from Wuhan University of Technology in 2013, and the M.E. degree from Huazhong University of Science and Technology in 2017. His current research interest is diluted magnetic semiconductor.

Qixin Wan received the B.E. degree from Nanchang University. He is currently pursuing the Ph.D. degree at Huazhong University of Science and Technology. His current research interest is wide bandgap semiconductor.

Jiangnan Dai received the B.E. degree from Hunan University of Science and Technology in 2002, and the Ph.D. degree from Nanchang University in 2007. Since 2010, he has been an associate professor at Huazhong University of Science and Technology, where he worked on photoelectric device based on wide bandgap semiconductor.

Jun Zhang received the B.E. degree from Jianghan University in 2012, and the Ph.D. degree from Huazhong University of Science and Technology in 2017. His current research interest is photoelectric device.

Feng Wu received the B.E. degree from Huazhong University of Science and Technology in 2012, and the Ph.D. degree from Huazhong University of Science and Technology in 2017. His current research interest is photoelectric device.

Shuai Wang received the B.E. degree from Huazhong University of Science and Technology in 2013. He is currently pursuing the Ph.D. degree at Huazhong University of Science and Technology. His current research interest is photoelectric device.

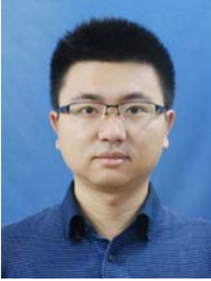

Hanling Long received the B.E. degree from Huazhong University of Science and Technology in 2014. He is currently pursuing the Ph.D. degree at Huazhong University of Science and Technology. His current research interest is photoelectric device.

Jingwen Chen received the B.E. degree from Beijing Jiaotong University in 2014. He is currently pursuing the Ph.D. degree at Huazhong University of Science and Technology. His current research interest is photoelectric device.

Cheng Chen received the B.E. degree from Wuhan Institute Of Technology in 2014, and the Ph.D. degree from Huazhong University of Science and Technology in 2017. His current research interest is photoelectric device.

Changqing Chen received the B.E. degree from Wuhan University in 1992, and the Ph.D. degree from University of Erlangen-Nürnberg in 2000. Since 2007, he has been a professor at Huazhong University of Science and Technology, where he worked on lighting emitting diode.